# INTERNATIONAL SOCIETY FOR SOIL MECHANICS AND GEOTECHNICAL ENGINEERING



This paper was downloaded from the Online Library of the International Society for Soil Mechanics and Geotechnical Engineering (ISSMGE). The library is available here:

https://www.issmge.org/publications/online-library

This is an open-access database that archives thousands of papers published under the Auspices of the ISSMGE and maintained by the Innovation and Development Committee of ISSMGE.

# Pore pressure dissipation in sand under cyclic stress triaxial testing

Dissipation post-liquéfaction de la pression interstitielle d'un sable soumis à un stress cyclique triaxial

Saizhao Du, Siau Chen Chian

Department of Civil & Environmental Engineering, National University of Singapore, Singapore, sc.chian@nus.edu.sg

ABSTRACT: Soil liquefaction has conventionally been studied as a pure undrained condition subject to cyclic shearing in the laboratory. However, in the field, ground settlement and expulsion of pore fluid in the form of sand boils are frequently observed in which conventional triaxial and simple shear apparatus are unable to replicate. In this study, a novel insight of coupled pore pressure generation and dissipation in liquefiable clean sand is discussed with the use of a modified cyclic triaxial testing setup. Stress-controlled cyclic triaxial tests with controlled pore water drainage is carried out to investigate "near-perfect undrained" conditions which is more representative to field conditions. This modification to the conventional triaxial setup provides the ability to study the effect of rate of pore water dissipation with the generation of excess pore pressure.

RÉSUMÉ: La liquéfaction du sol est classiquement étudiée en laboratoire comme un état non drainé pur soumis à un cisaillement cyclique. Cependant, sur le terrain, on observe fréquemment un tassement du sol et l'expulsion des fluides poreux formant des volcans de sable, dans lesquelles les mesures classiques triaxiales et de cisaillement simple sont difficilement repliables. Cette étude donne un nouvel aperçu du couplage de la génération et de la dissipation de la pression interstitielle dans un sable propre liquéfiable grâce à l'utilisation d'une configuration triaxiale cyclique modifiée. Des essais triaxiaux cycliques en stress contrôlés avec drainage contrôlé de l'eau interstitielle sont effectués afin d'étudier les conditions non drainées «presque parfaites » qui sont plus représentatives des conditions de terrain. Cette modification de la configuration triaxiale conventionnelle nous permet d'étudier l'effet de la vitesse de dissipation de l'eau interstitielle résultant de la génération d'une pression interstitielle excessive.

KEYWORDS: triaxial test, stress-controlled, near perfect undrained test, soil liquefaction, dissipation, stress path

### 1 INTRODUCTION.

Despite the study of soil liquefaction over the past half a century, its associated damage is still apparent in many recent major earthquakes in the 2016 Muisne (Franco et al. 2017), 2011 Tohoku (Chian et al. 2014), 2011 Christchurch (EERI, 2011), 2010 Maule (GEER 2010) and 2009 Padang (Wilkinson et al. 2012). Liquefaction induced failures include landslides, sand boils, excessive ground settlements, lateral spreading, and foundation failures. In the laboratory, soil liquefaction experiments were generally carried out to study excess pore pressure generation. In contrast, most of the above-mentioned liquefaction induced failures take place during the dissipation phase. Dissipation and redistribution of this shear induced pressure take place at a rate depending on the hydraulic conductivity and volume compressibility characteristics of the soil deposit and drainage conditions. When the rate of pore pressure generation and build up is significant, sandy materials loses a large portion of its strength, which may lead to liquefaction and breakdown of the soil structure. However, perfect undrained condition is rarely observed in the field following an earthquake as shown in the form of sand boils. Pore pressure dissipation is usually accompanied by rearrangement of particles, reconsolidation and a reduction in volume of voids, hence settlement of ground surface. It is likely that the liquefaction potential for these sands is substantially reduced by natural drainage in many cases.

With the introduction of performance-based design methodology in the recent decade, behavior of the soil becomes more important in optimising foundation design. To date, some excess pore pressure dissipation models have been developed based on results of centrifuge tests (Kokusho, 1999; Ha et al., 2003; Kim et al., 2006; Chian, 2015). However, few studies have been done to combine pore pressure generation and dissipation at the same time in a single cyclic triaxial test. This is the novelty of this study, where the near-perfect undrained

condition mimicking a better representation of the field is discussed relating to excess pore pressure generation and dissipation.

In this study, a series of stress-controlled cyclic triaxial tests at different stress amplitude and pore water flowrate is carried out. The amount of back water drained is monitored throughout the experiment for computation of instantaneous void ratio of the specimen. Table 1 shows the list of tests presented in this paper. The key test variables considered include cyclic stress amplitude and rate of pore water dissipation.

## 2 EXPERIMENTAL SETUP

Fine grained silica W9 sand supplied by Riversands Pty Ltd at Brisbane, Australia was used in this study. Typically used as a filtration medium, the sand's particle sizes are uniform (poorly graded). A percentage of 95% and above of the sand particles pass through #30 sieve (0.42 mm) and less than 5% of the particles pass through the #200 sieve (0.075 mm). Physical geotechnical properties of the sand are as follow:  $\Phi_{crit}$ =32°,  $D_{10}$ =0.22mm,  $D_{50}$ =0.26mm,  $D_{60}$ =0.3mm,  $G_{s}$ =2.65,  $e_{max}$ =0.86 and  $e_{min}$ =0.48.

The experiments were conducted on cylindrical specimens of 76 mm in height and 38 mm in diameter prepared using airpluviation method in a watertight rubber membrane with porous stones and filter paper on each ends. Each specimen was prepared at similar initial void ratios. A known weight of dry solids required to attain the target void ratio was weighed and divided into a few equal portions. The membrane was subjected to vacuum using an in-house mould to keep the membrane upright prior to pouring of sand at fixed fall height and similar flow rate. Both ends of the membrane were water-tight with rubber rings.

Initial void ratio is a highly sensitive parameter and will alter with a small change of mass in specimen. Hence mass control, density variation and void ratio non-uniformities has to be carefully controlled in this study. When applying air-pluviation method, specimens were prepared in a number of layers of

equal dry weight, and each layer was compacted to the same target density. This typically resulted in the lower portion of the specimen becoming denser than the global specimen density as compaction of each overlying layer also slightly densified the underlying layers (Papadimitriou et al., 2005). In this study, each sand layer was compacted slightly looser than the target global density so that the final density of each layer, accompanied with the effects of compaction of the successive overlying layers, would achieve a relatively uniform target global density throughout the specimen.

The dry sand specimen is subsequently saturated with deaired water via the back pressure inlet. The back pressure was increased gradually while maintaining the effective confining pressure at 20 kPa. The specimen was then consolidated isotropically (equal axial and radial stress) until a Skempton B-value of 0.95 or above was attained. Following saturation, the specimens were consolidated to a final effective isotropic confining pressure of 74 to 77 kPa before cyclic loading.

This marks the end of the preparation and the specimen ready for shearing under deviatoric loading. All drainage valves were initially closed to satisfy undrained condition requirement. In order to measure pore water flowrate, the amount of water flowing into or out of the specimen was monitored using another set of pressure controller was connected to the specimen. This permits computation of void ratio during excess pore pressure dissipation.

Table 1. Details of cyclic triaxial tests

Test ID	Test Parameters					
	e	Dr (%)	σ <sub>cyc</sub> (kPa)	σ' <sub>3</sub> (kPa)	q (mm³/s)	N <sub>cyc</sub>
NPUa1	0.696	44.3	0	76	5	35
NPUa2	0.695	44.7	0	76.2	20	15
NPUb1	0.702	42.8	44.1	75.8	5	73
NPUb2	0.691	45.7	44.1	77	20	18
NPUc1	0.698	43.7	70.5	77.4	5	93
NPUc2	0.693	45.2	70.5	76.6	20	21
NPUd1	0.711	40.3	88.2	74.8	5	109
NPUd2	0.701	42.9	88.2	75	10	55
NPUd3	0.694	44.7	88.2	76.7	20	24
NPUe1	0.710	40.6	132.3	76.4	5	136
NPUe2	0.694	44.8	132.3	77	20	28

In Table 1, e is the initial void ratio, Dr is initial relative density,  $\sigma_{cyc}$  is cyclic stress amplitude and  $\sigma'_3$  the effective confining pressure. q is the pore water flowrate and  $N_{cyc}$  is the number of cycles to dissipate all excess pore pressure from full liquefaction.

A series of separate permeability tests were conducted using the same sand at similar relative density and effective confining pressure. The coefficient of permeability of a fully saturated sand obtained using a constant head test in the same triaxial setup was about  $5 \times 10^{-4}$ m/s (or flow rate of about 7400mm³/s for a 38mm diameter specimen) under a pressure difference of 10kPa. In order to study the effect of pore water dissipation rate, three different flowrate levels were chosen as 5, 10 and 20 mm³/s, all of which were far lower than the permeability of the sand to ensure a near-perfect undrained condition.

Post-liquefaction coupled pore pressure generation and dissipation tests were initiated immediately following the end of cyclic loading phase where the specimen has attained and remained fully liquefied. The top end of the specimen was connected to a pressure controller to control rate of pore water discharge. The bottom end of the specimen was connected to a pore pressure transducer with no drainage allowed. This setup simulate a one-way drainage condition. These near-perfect

undrained tests were classified into two sets. The first set consisted of tests, without axial loading applied ( $\sigma_{cyc}$  =0) and drainage with controlled flowrate of 5 or 20 mm<sup>3</sup>/s, to simulate a pure excess pore pressure dissipation without cyclic shearing. They are labelled as NPU a1 and a2 in Table 1. For the second set, cyclic stress continues to be applied to the specimen while drainage of pore water was taking place (eg. NPU b1, c1, d1 and e1). This combined effect of cyclic stress loading and nominal drainage flowrate is "nearly undrained" but allow some pore pressure to dissipate which is more representative in the field where sand boils are observed. The duration of post-liquefaction pore pressure dissipation stage can extend as long as several hours (Tokimatsu and Seed, 1987), depending on the earthquake cyclic loading and permeability of the soil. These parameters are the focus of this study.

### 3 PORE PRESSURE DISSIPATION

Figure 1 show the results of excess pore pressure dissipation distribution for tests with a drainage flowrate of 5mm<sup>3</sup>/s for a wide range of shear strain amplitudes.

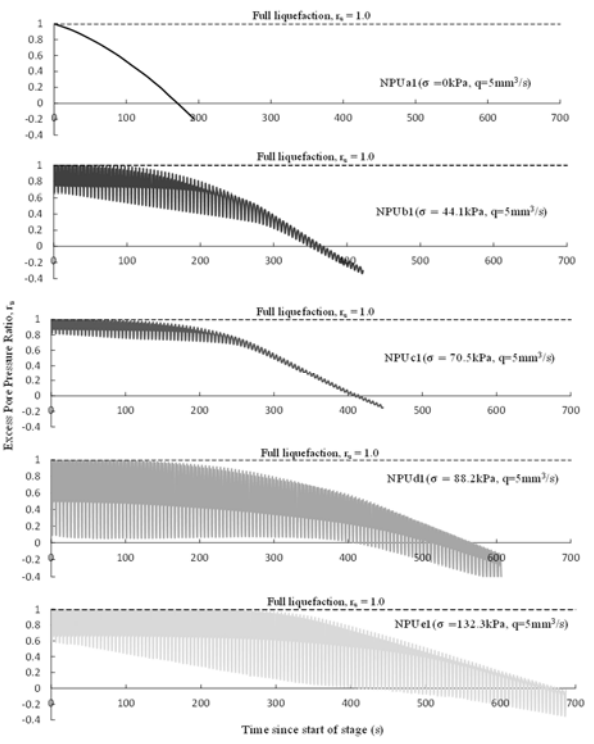


Figure 1. Excess pore pressure dissipation versus time at various stress amplitude (effect of  $\sigma_{cyc}$ )

In Figure 1, the excess pore pressure dissipation time histories followed a parabola trend resembling consolidation on self-weight. At greater cyclic shear amplitude, full liquefaction was maintained for longer. This is given the fact that the excess pore pressure dissipation equals to or less than the pore water pressure generation from the cyclic shearing, hence maintaining full liquefaction. However with continued drainage, an equilibrium will be attained as the sand gets compacted progressively with drainage of excess pore water. After that juncture, pore water pressure declines rapidly resembling the parabola as observed in Figure 1. The time required to attain this transition (i.e. the point where steepest slope of  $\frac{\Delta u}{t}$  is observed) is defined as the "transition duration".

Figure 2 shows excess pore pressure dissipation of the stress-controlled tests with stress amplitude of 88.2 kPa at

different rates of drainage. Similar trends in the relationship between pore pressure ratio and number of cycles can be observed when compared to those in Figure 1. With increasing drainage flow rate, time to arrive at the transition duration reduced dramatically. This is analogous to more rapid pore pressure dissipation in more permeable soils.

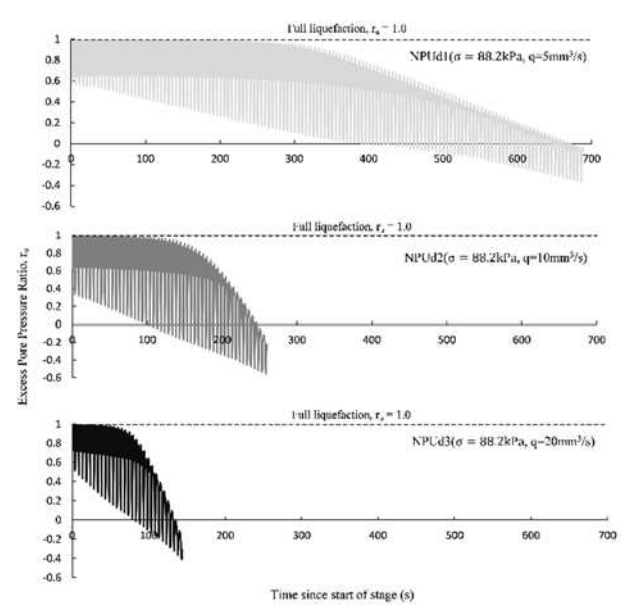


Figure 2. Excess pore pressure dissipation at different flow rate

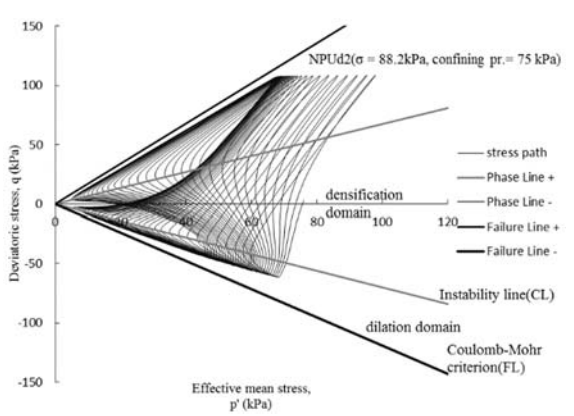


Figure 3. Stress path plot of Test NPUd2

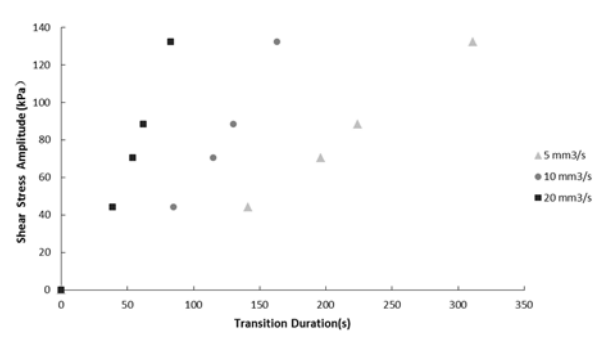


Figure 4. Shear stress amplitude versus transition duration at various flow rate

Another observation is the decreasing peak-to-peak amplitude of excess pore pressure with increasing number of cycles. Double frequencies of peaks also diminishes with increasing cycles in the later stage of all tests. In the early few cycles of cyclic loading with drainage, excess pore pressure

remained at high levels and the soil is dilating cyclically as its stress path continues to cross the phase transformation line as portrayed in Figure 3. This substantiates the observation of double frequency peaks in Figures 1 and 2. However, as the sand specimen is progressively compacted, the resistance to shear increases with greater retention of shear strength due to lower excess pore pressure. Therefore, the stress path departs from the origin and phase transformation line which is evident from the diminishing double frequency. Figure 4 shows a linear increase in transition duration with higher shear stress amplitude for different flowrate.

Figure 5 shows the difference in transition duration between different NPU tests as indicated in the legend of the plots. The rationale for subtracting the transition duration with NPUa1 and a2 is to separate the rate of excess pore pressure generation and dissipation. NPUa1 and NPUa2 are tests without cyclic shearing during dissipation. Hence they are deemed to exhibit excess pore pressure dissipation only. Therefore, subtracting the values from these tests would produce a net transition duration which is contributed solely by the excess pore pressure generation due to cyclic shearing. Higher shear stress amplitude tests produced a greater net transition duration, which is expected due to greater excess pore pressure generation. It is also observed that the gradient of the curves in Figure 5 remained linear for longer particularly in the case of higher stress amplitude. This is because full liquefaction was kept longer in those large stress amplitude tests. As the sand compacts further, excess pore pressure would eventually decline as supported by Figure 2. In order to explain this phenomenon, their excess pore pressure dissipations and void ratios were plotted as presented in Figure 6. The figure interestingly showed that the void ratio which marks the commencement of excess pore pressure decline was 0.69 for these tests, despite differing initial void ratios and stress amplitudes. This indicate that a critical void ratio exists where the sand has been compacted to a degree where excess pore pressure generation can no longer surpass the dissipation to support the high excess pore pressure in the sand. This finding may well provide guides on the minimum degree of densification of the sand as part of conventional soil liquefaction mitigation measures.

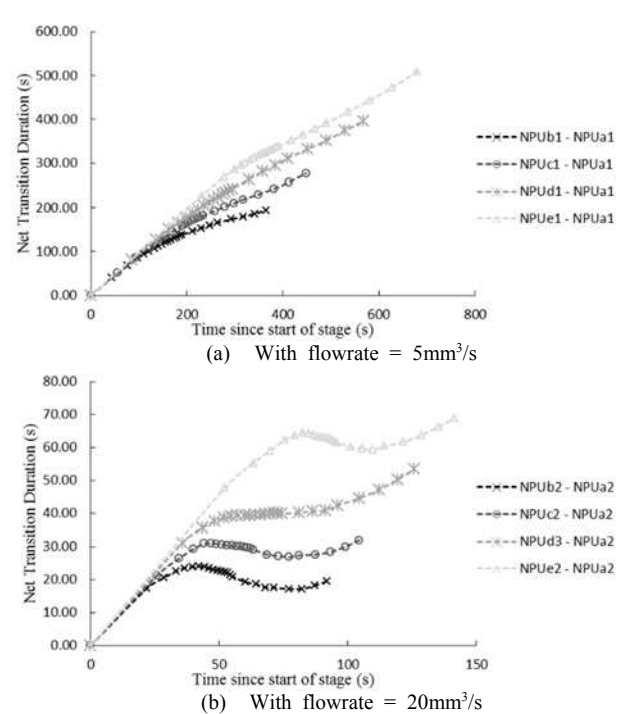


Figure 5. Effect of stress amplitude on pore pressure dissipation

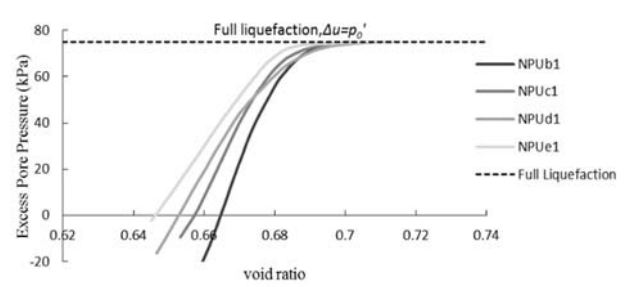


Figure 6. Pore pressure versus void ratio (with flowrate=5mm<sup>3</sup>/s)

### 5 CONCLUSION

A modified triaxial test system was adopted for studying the coupled generation and dissipation of excess pore pressure in clean sand subjected to cyclic loading and controlled drainage of pore water to represent the effects of pore water dissipation during cyclic shearing. Despite a flowrate of pore water way below the permeability of the sand (i.e. near perfect undrained condition), excess pore pressure would eventually decline as the sand compacts progressively. This is substantiated with pore water pressure time histories and stress path plots. It was also observed that the transition duration, where excess pore pressure commences its decline, is greater for specimens subject to higher cyclic shear stress amplitude, attributed to greater excess pore pressure generation. Greater flowrate of pore water also produces the same effect of more rapid dissipation of excess pore water pressure, analogous to a more permeable sand. A critical void ratio was found where excess pore pressure generation can no longer keep up with the dissipation despite subjected to high cyclic shear stresses.

### 6 ACKNOWLEDGMENT

The authors are grateful for the financial support from the Singapore Ministry of Education through the MOE Tier 1 grant R-302-000-081-133.

### 7 REFERENCES

Chian, S.C., Tokimatsu, K. and Madabhushi, S.P.G., 2014, Soil liquefaction-induced uplift of underground structures: Physical and numerical modeling. *Journal of Geotechnical and Geoenvironmental Engineering*, ASCE, 140(10), 04014057.

Chian S.C. Empirical Excess Pore Pressure Dissipation Model for Liquefiable Sands. 6th International Conference on Earthquake Geotechnical Engineering, 1-4 November 2015 Christchurch, New Zealand.

Earthquake Engineering Research Institute (EERI), 2011, The M 6.3 Christchurch, New Zealand. Earthquake of EERI February 22, 2011, EERI Special Earthquake Report.

Franco, G., Stone, H., Ahmed, B., Chian, S.C., Hughes, F., Jirouskova, N., Kaminski, S., Lopez, J., van Drunen, N.G. and Querembas, M., 2017, The April 16 2016 Mw7.8 Muisne earthquake in Ecuador – Preliminary Observations from the EEFIT reconnaissance mission of May 24 – June 7. 16th World Conference on Earthquake Engineering, Paper No. 4982.

Geoengineering Extreme Events Reconnaissance (GEER), 2010, Geoengineering reconnissance of the 2010 Maule, Chile earthquake, Report of the NSF Sponsored GEER Association Team.

Ha I. S., Park Y. H., and Kim M. M. 2003. Dissipation pattern of excess pore pressure after liquefaction in saturated sand deposits.
Transportation Research Record. 1821, *Transportation Research Board, Washington, D.C.*, 59–67.
Kim S. R., Hwang Ji., Bao Y., Ko H.Y., Kim M.M.2006. Comparison of

Kim S. R., Hwang Ji., Bao Y., Ko H.Y., Kim M.M.2006. Comparison of 1-g and centrifuge model tests for liquefied sands. *Proc. 6th Int. Conf. on Physical Modelling in Geotechnics*, 18–22. Papadimitriou, A. G., Dafalias, Y. F., and Yoshimine, M., 2005, Plasticity Modeling of the Effect of Sample Preparation Method on Sand Response, *Soils Foundations*, Vol. 45, No. 2, pp. 109–123.

Tokimatsu, K. and Seed, H. B., 1987, Evaluation of settlement in sands due to earthquake shaking. *Journal of Geotechnical Engineering*, ASCE, 113(8), p. **861-878**.

Wilkinson, S.M., Alarcon, J.E., Whittle, J. and Chian, S.C., 2012, Observations of damage to building from Mw 7.6 Padang earthquake of 30 September 2009. Natural Hazards, 63, p. 521-547.